DEGREE PROJECT IN VEHICLE ENGINEERING,
SECOND CYCLE, 30 CREDITS
STOCKHOLM, SWEDEN 2020

ONERA
THE FRENCH AEROSPACE LAB

CentraleSupélec

Flight Mechanics of an Airship

Flygmekanik för ett Luftskepp

PIERRE MERLET

KTH ROYAL INSTITUTE OF TECHNOLOGY
SCHOOL OF ENGINEERING SCIENCES

Authors

Pierre MERLET
merlet@kth.se
Aerospace Engineering
KTH Royal Institute of Technology

Place for Project

ONERA, Lille, France
January - June 2020

Examiner

Ulf Ringertz
Teknikringen 8, Rum 6620
KTH Royal Institute of Technology„ Stockholm, Sweden

Supervisor

Dominique Farcy
Aerodynamics, Aeroelasticity, Acoustics Department - DAAA - Unit ELV
ONERA, Lille, France

Ulf Ringertz
Teknikringen 8, Rum 6620
KTH Royal Institute of Technology, Stockholm, Sweden

Flight Mechanics of an Airship

Pierre Merlet*
KTH, Stockholm, Sweden - June 2020

Luftskepp var mycket populär för 90 år sedan, till exempel med tyska Zeppelinare. Nu är de tillbaka av flera skäl, som deras låga energiförbrukning.

Men det finns fortfarande många problem att hantera som deras känslighet för vindbyar.

Dessutom behöver luftskeppen fler studier för att förbättra sina flygegenskaper och vindkänslighet.

Detta examsarbete, utfört vid den franska institutionen ONERA i Lille, studerar ett specifikt luftskepp som är 5 m långt och 1.7 m brett. Först, studeras luftskeppet utan vind för att bestämma aerodynamiska data och tröghetsegenskaper. Sedan genomförs experiment där modellen utsätts för vindbyar.

Airships were very popular 90 years ago with, for example, german Zeppelins. Now they are back for several reasons, like their low energy consumption.

But there are also still many problems to deal with like their sensitivity to wind gusts.

In addition, the airships need more studies to improve their flight mechanics and sensitivity to the wind.

This degree project, done with the French Aerospace Lab ONERA in Lille, studies a specific airship which is 5 m long and 1.7 m wide. First, the airship is studied without wind to determine aerodynamic coefficients and added masses. Then, the model is confronted to experiments with wind gusts.

I. Nomenclature

l	Length of the airship [m]	m_{Fij}	Added masses/inertias of the fins [kg / kg.m^2]
L_{ref}	Length of reference of the hull [m]	$[x_{cv}, y_{cv}, z_{cv}]$	Center of volume coordinates (body frame) [m]
D	Max diameter of the airship's hull [m]	$[x_{cg}, y_{cg}, z_{cg}]$	Center of gravity coordinates (body frame) [m]
R	Hull's radius [m]	$[x_p, y_p, z_p]$	Main thrust center's coordinates (body frame) [m]
$[a_i, b, c]$	Semi-axis of the ellipsoid [m]	$[x_f, y_f, z_f]$	Fin thrust center's coordinates (body frame) [m]
S_{ref}	Surface of reference of the hull [m^2]	$[\phi, \theta, \psi]$	Euler angles (roll, pitch, yaw) [rad]
S_f	Surface of reference of the fins [m^2]	α	Angle of attack [rad]
V_{ref}	Volume of the airship's hull [m^3]	β	Side-slip angle [rad]
δ_E	Elevator's angle [rad]	C_L	Lift coefficient (inertial frame)
δ_R	Rudder's angle [rad]	C_D	Drag coefficient (inertial frame)
μ_p	Main thrust's angle [rad]	C_m	Pitch moment coefficient
δ_T	Main thrust's command [0:1]	U	Airspeed [m.s-1]
δ_{T_f}	Fin thrust's command [-1:1]	$[u \quad v \quad w]$	Airspeed's components (body frame) [m.s^{-1}]
m	Total mass of the airship [kg]	$[p \quad q \quad r]$	Rotational airspeed's components (body frame) [m.s^{-1}]
M	Mass matrix	T	Thrust [N]
I_{ij}	Mass moment of inertia [kg.m^2]	B	Buoyancy [N]
k_i	Lamb's coefficients [-]	g	Gravity constant [m.s^{-2}]
K_i	Added masses/inertias of the hull [kg / kg.m^2]	ρ	Gas density [kg.m^{-3}]

*Master student, merlet@kth.se

II. Introduction

With the growing interest given to the sustainable development and renewable energies, airships are getting interests for a second time in their history. Indeed, they were popular in the beginning of the XXth century with the Zeppelins and the US Navy airships.

Nonetheless, with the development of airplanes and the Hindenburg disaster, the development of airships was progressively abandoned.

Since the beginning of the XXIth, several companies have started again to build airships and develop the technology. As they use Archimedes force to lift themselves, their energy consumption is way lower than the one of an airplane or an helicopter. Then, they can offer an efficient alternative for missions not necessitating a fast or agile vector.

In order to make the development of these new airships, the flight's dynamics of airships have to catch up with the one from usual Heavier-Than-Air aircraft.

This paper aims to provide a method to model the flight mechanics of an airship in a calm atmosphere at first, and next with the influence of wind gusts. To do so, the model established is confronted to the experiment by using a 5 m long airship in a free flight laboratory in ONERA premises.

This project is realised as part of a master thesis for the Aerospace Master from KTH-Stockholm and a final-year internship for the Engineering degree from Centrale Paris. The internship has been conducted in the ONERA premises of Lille.

In this project the airship is assumed to be rigid and thus aeroelastic effects are neglected. Then the influence of ballonets will not be studied, meaning that the altitude's variation and internal transfer of mass are neglected. Also, the center of gravity and of buoyancy are assumed to lay in the same longitudinal plan and the curvature of the Earth is neglected.

III. Method

A. Airship's structure

An airship has the peculiarity of being a buoyant object. It uses aerostatic forces to generate its lift. Indeed, the hull, largest part of the airship, is made of an envelope filled by a Lighter-Than-Air (LTA) gas which lift the airship thanks to Archimeds force.

Then, motors are added to manoeuvre it and control its displacement independently of the wind. The motors are typically attached to the gondola, the box attached to the bottom of the hull. It contains the payload and the tools needed for the flight. At the rear of the hull are attached fins. These helps to manoeuvre the airship with the aerodynamic forces they create.

$$B = V_{ref}\,(\rho_{air} - \rho_{LTA})g \tag{1}$$

The hull is modeled as 2 joined semi-ellipsoid of revolution which cross sections are discs (cf part IV.A).

B. Frames of reference

For airships, the equations are usually solved in the body's frame which origin is at the center of volume as it can be seen in the Figure 1. The center of volume is assumed to be the center of the ellipsoid used to model the airship's hull. For most airships, two semi-ellipsoids are used.

The position of the center of volume lies on the two axes of symmetry of the hull, assumed to be a body of revolution, and its position in the x direction can be computed analytically [1].

To get the trajectory of the airship, the Earth's frame is used. The conversion from the body's frame to the Earth's frame is done thanks to the matrices of rotation using the Euler's angles ϕ, θ and ψ.

To avoid the singularities that can occur when the airship is oriented at a pitch angle of $\pm 90°$ for example, the quaternions are used for the dynamic. Using four parameters to describe the three usual rotations, they prevent the appearance of singularities [2, 3].

Then, the actuators angles are defined according to the Figure 1. One can note that the actual disposition of the tailplanes is in a cruciform disposition, i.e. 2 vertical and 2 horizontal fins.

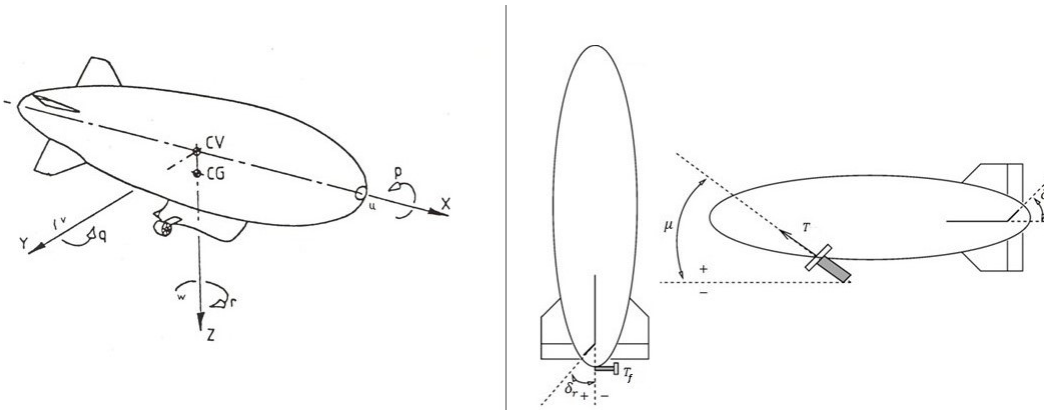

Fig. 1 Body axes system of the airship showing C.V, C.G and linear (u, v, w) as well as angular (p, q, r) velocities around the X, Y, and Z axes respectively and the actuators definitions. [4, 5]

C. Mass matrix

1. Added masses

One of the issue of the airships compared to usual aircraft is the aerodynamic effect of added masses. For usual aircraft the mass of the displaced air by the object can be neglected in regard to the mass of the object itself. However, for an airship, the mass of the displaced air can be quite close to the mass of the airship and cannot be neglected.

The added masses and inertias can be understood as the forces due to an incompressible and instationnary flow and will considerably modify the behaviour of the object [6].

In the specific case of ellipsoid shapes, analytical formulas exist to determine these added masses and inertias for the hull of the airship. These formulas are expressed in the body frame of the airship and then used to fill the mass matrix.

Considering an ellipse with two semi-axis and a circular cross-section, the added masses and inertias coefficients, also known as the Lamb's coefficients k_1, k_2 and k_3, are given by analytical formulas [7].

Following Nielsen's method [8], the added masses and inertias of the fins, m_{Fij}, were also added. Indeed, they can represent up to approximately 40% of the total added mass or inertia for certain term like the masses corresponding to a displacement in the lateral plan.

2. Complete Mass Matrix

The mass matrix contains both the usual terms of masse and inertia and the ones due to the phenomena of added masses. Then, the complete mass matrix is obtained by summing all the contributions.

For the hull of the airship, the mass of the LTA gas, helium here, can be considered as an ellipsoid to be able to use the analytic formulas. For the envelop of the hull, the inertias can be computed from a surface integral. The gondola and fins are treated in a classic way thanks to the Huygens's theorem.

$$M = \begin{bmatrix} m+K_1 & 0 & 0 & 0 & mz_{cg} & 0 \\ 0 & m+K_2+m_{F22} & 0 & -mz_{cg} & 0 & mx_{cg}+m_{F26} \\ 0 & 0 & m+K_2+m_{F33} & 0 & -mx_{cg}+m_{F35} & 0 \\ 0 & -mz_{cg} & 0 & I_{xx}+m_{F44} & 0 & -I_{xz} \\ mz_{cg} & 0 & -mx_{cg}+m_{F35} & 0 & I_{yy}+K_3+m_{F55} & 0 \\ 0 & mx_{cg}+m_{F26} & 0 & -I_{xz} & 0 & I_{zz}+K_3+m_{F66} \end{bmatrix} \quad (2)$$

In the Equation 2, the terms K_i correspond to the added masses of the hull, while m is the total mass of the airship and I_{ij} the mass moment of inertia of the whole airship in the body frame.

D. Aerodynamic coefficients

The aerodynamic coefficients for the airship contain the usual ones for lift and drag and additional ones due to the airship's specific structure.

$$V_{ref} = \frac{4\pi}{3}abc \quad ; \quad S_{ref} = V_{ref}^{\frac{2}{3}} \quad ; \quad L_{ref} = V_{ref}^{\frac{1}{3}} \tag{3}$$

In the following parts, all coefficients are adimensionned using the volume of reference V_{ref}, the surface of reference S_{ref} and the length of reference L_{ref} as they are given in the Equation 3.

The forces described by the aerodynamic coefficients given here are all expressed in the airship's frame.

1. Drag

According to Khoury, [9], the total drag of the airship is approximately equal to twice the axial drag of the hull. This estimation is based on the comparison of the results obtained on several airships. Even if largely smaller than the hull, other's part drag is relatively high due to all the bearings and appendices they present.

$$C_{D_0H} = \frac{C_F}{S_{ref}}\left[4\left(\frac{l}{D}\right)^{\frac{1}{3}} + 6\left(\frac{l}{D}\right)^{-1.2} + 24\left(\frac{l}{D}\right)^{-2.7}\right] \tag{4}$$

An estimation of the axial drag coefficient for the hull is given by the Equation 4, with C_F a friction coefficient depending on the Reynolds number [10].

Besides the axial drag, the cross-flow drag has also a non-negligible influence. In order to evaluate the cross-flow drag, the impact of the gondola, which area is very small in regards to the one of the hull, is neglected here.

$$C_{Dc} = -\frac{1}{S_{ref}}\left(C_{Dch}J_1 S_{ref} + C_{Dcf}S_f\right) \tag{5}$$

The cross-flow drag coefficient given in the Equation 5 is right for both directions Y and Z. In the Equation 5, the coefficient C_{Dch} and C_{Dcf} correspond to the drag coefficient of respectively a cylinder and a plate in a transverse flow [11, 12]. The surface S_f refers to the fin's reference area as defined by Khoury, [9], and J_1 is analytically obtain [1].

2. Lift

As the hull is symmetric, it would at first not create lift according to perfect fluid theory. However, as the flow tends to separate at the rear of the hull, a lifting force is created. This force is generally expressed from the Munk moment (cf part III.D.3), accounting for the incidence effect on the hull distributed pressure.

$$C_{Lmunk_\alpha} = \frac{dC_{L_{munk}}}{d\alpha} = (k_2 - k_1)\eta_k I_1 \tag{6}$$

An expression of the Munk coefficient is given in Equation 6 with η_k the hull efficiency and I_1 a term accounting for the ellipsoid geometry [1].

Then the lift generated by the fins have to be computed as well. The main issue for the corresponding coefficient is to obtain the fin efficiency η_f. This efficiency models the influence of the hull on the forces created by the fins.

$$C_{Lfin} = -\frac{1}{2}C_{L_\alpha}\frac{S_f}{S_{ref}}\eta_f \alpha_f \quad ; \quad \eta_f = (1 + \frac{R^2}{s^2}) \tag{7}$$

The lift coefficient due to the fins can be expressed as shown in the Equation 7, [13], with the fin efficiency given as a function of the radius of the hull and the fin's aerodynamic centre height at the fin's aerodynamic centre longitudinal position.

The angle of attack seen by the flap is assumed to be the same as the one seen by the airship in general, i.e. $\alpha_f = \alpha$.

In the Equation 7, the general lift coefficient used is the 3D lifting coefficient of a low aspect-ratio wing. This coefficient can be obtained from the 2D lifting coefficient of the same wing using the Lifting-Line theory [14].

As the fins have flaps to manoeuvre the airship, the Equation 7 is slightly modified to modify their effect.

$$C_{Lflap} = -\frac{1}{2}C_{L_\delta}\frac{S_f}{S_{ref}}\eta_f \delta_{flap} \quad ; \quad C_{L_\delta} = \tau\eta_d k_{3D} C_{L_\alpha} \tag{8}$$

The coefficient C_{L_δ} in the Equation 8 can be determined from the coefficient C_{L_α} thanks to the flap efficiency η_d, which takes into account the decreasing efficiency of the flap as its deflection increases, the theoretical effectiveness factor τ and a 3D coefficient k_{3D}, function of τ and the aspect-ratio, [15].

3. Moments

The previous forces also generate a moment at the airship centre of volume.

$$C_{M_{Dc}} = -\frac{1}{V_{ref}}\left(C_{Dch}J_2V_{ref} + C_{Dcf}S_f l_{f2}\right) \tag{9}$$

The cross-flow drag moment coefficient is obtained from the Equation 9 where l_{f2} is the distance from the nose to the mid-chord of the fins.

For the lift generated by the fins and their flaps, the moment is the product of the force by the distance from the center of volume to the aerodynamic center of the fins, noted l_{f1}.

$$C_{Mmunk_\alpha} = \frac{dC_{M_{munk}}}{d\alpha} = -(k_2 - k_1)\eta_k I_3 \tag{10}$$

For the Munk moment, the geometry of the hull intervenes as detailed in the Equation 10 to get the moment due to the lift generated by the hull, I_3 accounting for the ellipsoid geometry [1].

In addition to these moments, an airship experiences a pitching moment following a linear function of the pitch rate and a yawing moment following the same function of the yaw rate. The two coefficients describing those moments are equal as the airship has two symmetry axes: $C_{mq} = C_{nr}$.

$$\Delta C_{mq} = C_{L_\alpha cyl}\frac{x^2}{V_{ref}}dS \quad ; \quad \Delta\alpha = \frac{xq}{U} \tag{11}$$

This two coefficients are obtained by integrating over the length of the hull the moment due to the lift generated by a pitch or yaw rotation of the hull on the element of surface dS, Equation 11. $C_{L_\alpha cyl}$ is the lifting coefficient of a finite cylinder in an axial flow [16]. Once the integration has been done, the fin's contribution has to be added. To do so, the lift due the angle $\Delta\alpha$ on the fins is used to get the fin's part to this moment.

Computed this way, the two corresponding moments are obtained by multiplying the coefficients C_{mq} and C_{nr} by the pitch rate q and yaw rate r respectively.

4. Aerodynamic vector

Using the aerodynamic coefficients provided in this section, the aerodynamic vector A can be constructed.

$$A = \begin{bmatrix} \frac{1}{2}\rho_{air}U^2S_{ref}\left[2C_{D_0H}cos(\alpha)^2cos(\beta)^2 + C_{Lmunk_\alpha}\left[sin(2\alpha)sin(\frac{\alpha}{2}) + sin(2\beta)sin(\frac{\beta}{2})\right]\right] \\ \frac{1}{2}\rho_{air}U^2S_{ref}\left[C_{Lmunk_\alpha}cos(\frac{\beta}{2})sin(2\beta) + C_{Lfin}(\beta_f)sin(2\beta) + C_{Dc}sin(\beta)sin(|\beta|) - C_{Lflap}(\delta_R)\right] \\ \frac{1}{2}\rho_{air}U^2S_{ref}\left[C_{Lmunk_\alpha}cos(\frac{\alpha}{2})sin(2\alpha) + C_{Lfin}(\alpha_f)sin(2\alpha) + C_{Dc}sin(\alpha)sin(|\alpha|) + C_{Lflap}(\delta_E)\right] \\ 0 \\ \frac{1}{2}\rho_{air}U^2V_{ref}\left[C_{Mmunk_\alpha}cos(\frac{\alpha}{2})sin(2\alpha) + C_{Lfin}(\alpha_f)l_{f1}sin(2\alpha) + C_{M_{Dc}}sin(\alpha)sin(|\alpha|) + C_{Lflap}(\delta_E)l_{f1} - C_{mq}q\right] \\ \frac{1}{2}\rho_{air}U^2V_{ref}\left[-C_{Mmunk_\alpha}cos(\frac{\beta}{2})sin(2\beta) - C_{Lfin}(\beta_f)l_{f1}sin(2\beta) - C_{M_{Dc}}sin(\beta)sin(|\beta|) + C_{Lflap}(\delta_R)l_{f1} - C_{nr}r\right] \end{bmatrix} \tag{12}$$

The Equation 12 gives the aerodynamic vector for the airship in its body frame.

E. Static Forces

An airship faces two static forces: the gravity and the buoyancy. These two forces are vertical in the Earth's frame. The gravity acts at the center of gravity of the airship while the buoyancy acts at the center of buoyancy. Here, it is assumed that the center of buoyancy is located at the same location as the center of volume.

Then, only the acceleration of gravity creates a pitch moment on the airship and the forces and moments just need to be written in the body's frame.

F. Propulsion

An airship have motors attached to the gondola to manoeuvre in a calm atmosphere or even against the wind. The motors are usually using a rotor to propel the airship and can be oriented. Moreover, to avoid creating a rolling moment, the motors are usually centered on the longitudinal plan of symmetry of the airship.

$$P = T(\delta_T) \begin{bmatrix} cos(\mu_p) \\ 0 \\ sin(\mu_p) \\ 0 \\ sin(\mu_p)x_p + cos(\mu_p)z_p \\ 0 \end{bmatrix} + T_f(\delta_{T_f}) \begin{bmatrix} 0 \\ 1 \\ 0 \\ -z_f \\ 0 \\ x_f \end{bmatrix} \tag{13}$$

In this study, the coordinates of the main propulsive center are given by $CP(x_p, y_p = 0, z_p)$. This simplifies the propulsion matrix P as shown in the Equation 13 where T is the total main thrust and δ_T the input given on the thrust in between 0 and 1. The orientation of the motors around the y-axis is described by μ_p (see Figure 1).

Besides, the main propulsive system, the airship is equipped with a small propeller on its bottom fin at the position $C_f(x_f, y_p = 0, z_f)$. The same methodology as for the main propeller is used. Nonetheless, the coefficient δ_f is given in between -1 and 1 to account for the blade being able to turn in the two directions.

For the main propellers, the thrust depends on the velocity of the airship. Indeed, the propeller system efficiency increases with the airspeed once the thrust has reached a certain force.

$$\eta_{prop} = \frac{2}{1 + \frac{u_{out}}{u_{in}}} = \frac{2}{1 + \sqrt{1 + \frac{T}{\frac{1}{2}\rho_{air}u^2 S}}} \tag{14}$$

The efficiency of the propellers is computed thanks to the Equation 14 based on the equations of an helicopter rotor in axial climbing flight [17].

G. Inertial forces

These terms are due to the choice of the frame of reference. As the forces and moments are expressed in the body frame, which is moving in regards to the inertial frame, new terms appears when Newton's second law is applied. These terms are here modeled as forces and moments [13].

H. Wind Forces

Due to their relatively large size for their low weight, airships are very sensitive to winds and more specifically gust winds. Moreover, as airships are usually long, the wind's effect can be located only on part of its body. This makes it necessary to use a model describing the spatial distribution of the wind along the airship's length.

In this section, the wind force considered is the one created by the wind tunnel: a lateral constant wind with no angular velocity.

To compute the force due to the wind, the aerodynamic forces generated in the calm atmosphere and the ones in the windy ones are supposed to be independent. As a result, it is assumed they can be summed to obtain the total aerodynamic force.

Consequently, the only modification to apply to the calm atmosphere model is to replace the airship's airspeed by the airship's relative airspeed to the wind for the propulsion and inertial forces.

Then, the wind force is separated with the hull and the tail's fins contributions.

For the hull, the gust airspeed is assumed to be low compared to the forward airspeed of the airship to be able to use a slender body theory. This hypothesis might however not always be verified in the experiments.

$$\frac{dF_{wind}}{dx} = \frac{1}{2}\rho_{air}u^2 S_{ref}\left(4\pi\frac{l^2}{S_{ref}}\frac{R}{l}\frac{dR}{dx}\frac{v}{u}\right) \tag{15}$$

Then, the Equation 15 gives the local transverse force on a section dx of the airship's length. In the Equation 15, the airspeed u refers to the forward airspeed, i.e. the airship's airspeed along its X-axis, and v to the lateral wind velocity, i.e. along the airship's Y-axis or Z- axis [18]. The total force and momentum created by the wind are found integrating the local force over the airship's length l.

Besides, as the airship begins to rotate because of the wind, part of the lateral wind will become a headwind or a tailwind. This is modeled using the previous drag model for a forward airspeed.

Considering the tail's contribution, a simple drag model for a plate is used, with the same drag coefficient as in Equation 5.

IV. The airship

A. Geometry

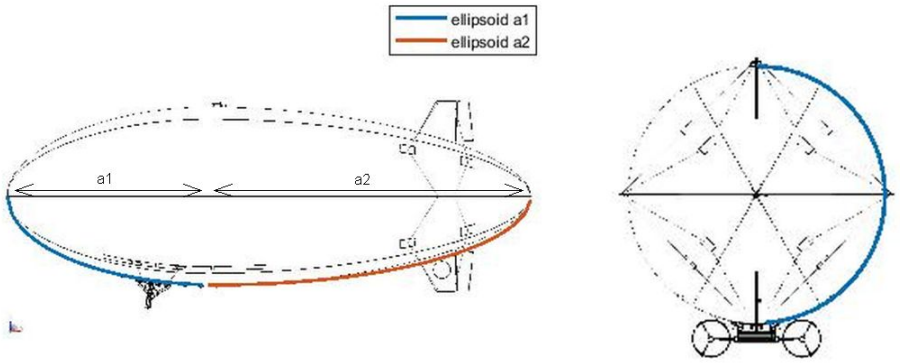

Fig. 2 Airship's geometry.

The airship used for the experiment is the 5 m Outdoor RC Blimp from Aero Drum Ltd, in Serbia. The purpose of this airship is usually to do advertisement in stadium or in low-wind places. It is eventually used for aerodynamic experiments by universities or research institutes.

Table IV.A Airship characteristics.

Length $[m]$	5	Max Diameter $[m]$	1.7
Volume $[m^3]$	7.5	Mass $[kg]$	~ 8

The main characteristics of the airship are summed up in the Table IV.A.

This airship is powered by 2 rotors fixed on the gondola. The 4 fins are disposed in a cruciform configuration, the bottom one having a small rotor incorporated. The 4 fins have the same sweep angle at the leading edge: $\Lambda = 27°$. The two motors are each running on a battery while a third one is used for the radio-controlled system.

As most airship, the shape of this airship is close to an ellipsoid. As it can be seen in Figure 2, the ellipsoid described by the two semi-axis $a_1 = 2$ m and $a_2 = 3$ m with $b = c = 0.85$ m, gives a good approximation of the hull geometry. It also provides us with a volume of 7.6 m^3 and a outer surface of 22.6 m^2.

From the airship's geometry, the positions of the center of volume and the center of gravity can be determined. In this analysis, the center of buoyancy is assumed to be located at the same position as the center of volume.

As the position of the light system in the envelope is unknown, static tests were used to balance the center of gravity of the envelop. Once this center is known, the rest of them is obtained by simple computations.

Besides, the airship can be trimmed, both in order to get a null pitch angle and a null total buoyancy, thanks to small masses added at the nose and the rear of the airship.

B. Air properties

An other important parameter to consider for the efficiency of the airship is the density of the LTA gas used. For this airship, Helium He was chosen. It might not be as efficient as the Hydrogen H, but it is much safer, explaining its popularity among most manufacturers nowadays. Although, for an exact model, the temperature would need to be adapted to the current situation. Indeed, the variation of the density of the Helium and the air is not equal with the temperature. As the temperature increases, the buoyancy of the airship tends to decrease. For example, going from 15°C to 18°C, the airship would lose a hundred grams of net buoyancy.

C. Propulsion system

The airship is equipped with two main propellers fixed on the gondola. Each of them is running on a Li-Po battery with a voltage of 11.1 V and a 0.3 ohms internal resistance. They are controlled through a Electronic Speed Control (ESC) system which efficiency is estimated to $\eta_{ESC} = 0.85$, [19].

The motor used for the main propulsion is a brushless motor. The motor is equipped with a 5:1 gear reduction to limit the propeller rotational speed and its efficiency is estimated to $\eta_{motor} = 0.89$.

The propeller installed is made of carbon and its efficiency is computed thanks to the Equation 14.

$$T = \frac{1}{u + u_i} \eta_{prop} \eta_{motor} \eta_{ESC} \frac{(\frac{\delta_T V_{motor}}{5})^2}{R_{battery}} \tag{16}$$

From the components data and assuming the motors are controlled with a Pulse Width Modulation signal modulating the voltage, the thrust obtained by one propeller and motor is obtained from the Equation 16 where δ_T is the control parameter for the voltage input V_{motor} and then the thrust, and u_i the inflow airspeed [17].

The bottom-fin motor is a brushed motor able to rotate in the two directions running on a separated battery.

V. Results

A. Aerodynamic model

The first block of the model tested is the aerodynamic one as it is the first to be validated.

To do so, the forces coefficients were plotted with the Angle of Attack (AoA) to be able to compare them with others experimental results. Such results can be found in studies on the YEZ-2A or ZHIYUAN-1 airship, [4, 20]. Also the forces are here defined in the inertial frame to match the other experiments.

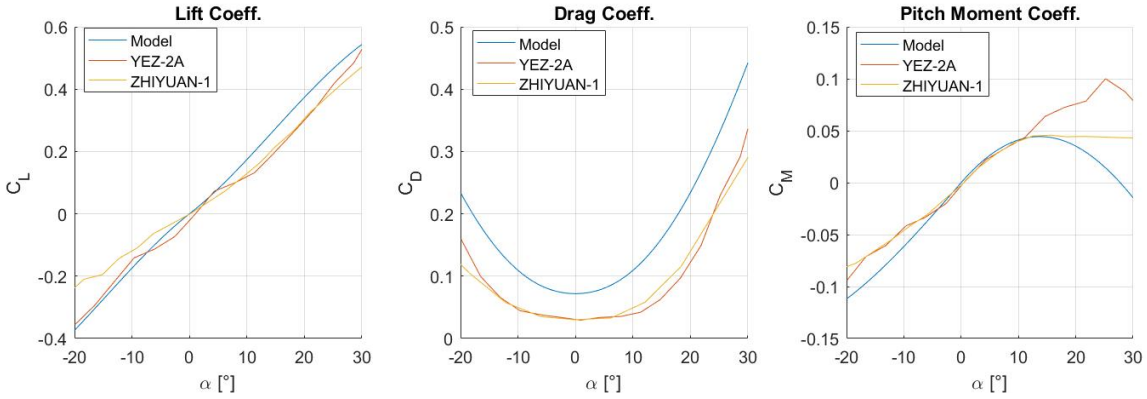

Fig. 3 Aerodynamic coefficients in the inertial frame compared to the YEZ-2A and ZHIYUAN-1 data.

The results obtained with the current model are shown in the Figure 3. It can be seen that the lift, drag and pitch moment coefficient curves seems to be similar to the one from the previous sources. Nevertheless, it can be noted that the drag appears to be higher. It can be explained by the low fineness ratio of the considered airship. Then, the friction drag accounts for more than the usual ratio of the total drag.

B. Propulsion model

In order to model properly the forward flight of the airship, its propulsion performance need to be tested.

To do so, the Equations describing the propulsive system of the airship were used to compute the thrust generated by one propeller. Using this modelisation of the thrust, a maximal speed of 3.8 m.s^{-1} was estimated thanks to a 1D model.

VI. Experiments

A. Static Tests

1. Roll and pitch oscillations

To compare the inertias in regards to the X-axis and Y-axis, a static test can be done. The airship is placed with a non-zero roll or pitch angle. Once free, it oscillates back to its equilibrium. The decay rate provides with the aerodynamic damping when there is no forward speed while the pseudo-period gives the considered inertia.

To do so, the hypothesis of small angles oscillations is made, and for the experiment the center of gravity is assumed to be located at the center of volume of the hull, i.e. $x_{cg} = 0$. The damping is modeled as a function of the roll or yaw speed.

$$I_j \ddot{X}_j - C_{j0} \dot{X}_j - mg z_{cg} X_j = 0 \quad ; \quad \lambda = \frac{C_{j0}}{2I_j} \pm i \frac{\sqrt{-(\frac{C_{j0}}{I_j})^2 + 4\frac{mg}{I_j} z_{cg}}}{2} \quad with \quad \begin{cases} j = x & roll \\ j = y & pitch \end{cases} \tag{17}$$

This experiment allows to add the coefficient C_{j0}, as described in the Equation 17, to the model for the roll and pitch oscillations and to confirm, or not, the two inertias.

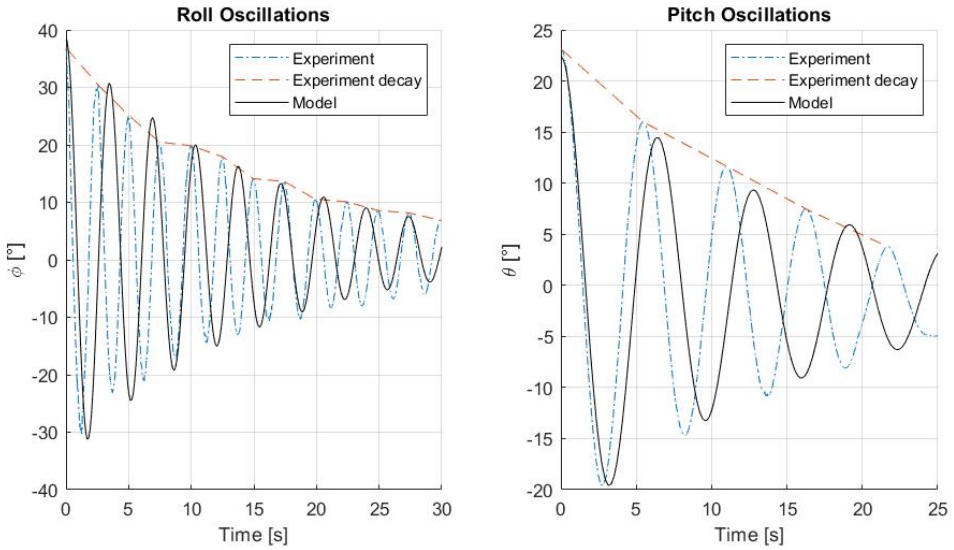

Fig. 4 Comparisons of the roll and pitch oscillations from the updated model and the experiment.

As it can be seen from the Figure 4, the error on the period of the oscillations is quite significant, with an experimental period around 1 second shorter than the one computed by the model. Assuming only the inertia is the unknown, it would give an inertia respectively 70% and 45% higher in the model than in the experiment for the rolling and pitching oscillations and therefore a non negligible error.

However, if the vertical position of the center of gravity z_{cg} is considered as the unknown, a difference of 20 cm with the modeled one, which is $z_{cg} = 29$ cm, would fit the experimental results.

As a result, the period is sensitive to both possible unknowns. The actual result might be then a small difference with both the inertia and the center of gravity's position.

Concerning the damping effect, as the effect was not modeled yet, the coefficients were directly added to the Equation 12 as modeled in Equation 17. The values obtained were $C_{x0} = -0.85$ N.m.s and $C_{y0} = -2.9$ N.m.s.

2. Propulsion

During the first experiments, even if attempts to measure a maximal speed were not successful, the expected maximal speed was estimated around 4 m.s^{-1}. This is then supporting the current propulsion model.

A deceleration test was also performed to confirm the drag coefficient C_{D_0H} but the recording time was too short to see a significant deceleration and get an estimation from it.

For the bottom-fin propeller, an other test was held: with the airship at the equilibrium, the maximal thrust of the motor was delivered and the time to complete a 180° rotation counted. This test was used to model the rotational speed of the airship for a given thrust.

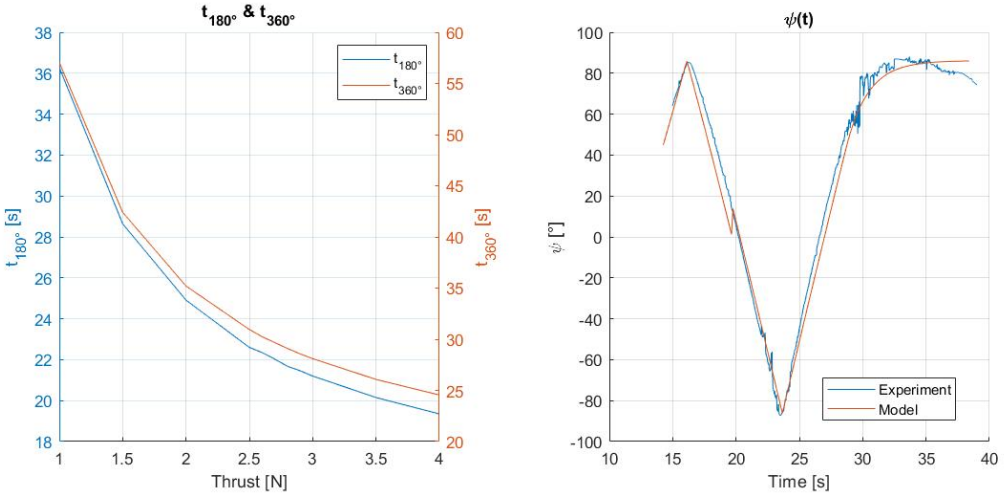

Fig. 5 Time to complete a rotation as a function of the thrust and comparison of the model with the experiment for $T_f = 2.95$ N.

As the times to complete a 180° and a 360° rotation were counted to be respectively 9 and 16 seconds, a first estimation of the thrust was 3 N from the model in Figure 5a. Comparing the model and the experiment result in the Figure 5b, the maximal thrust generated by the bottom-fin propeller was refined to 2.95 N.

B. Wind tests

The wind tunnel used for the experiments is made of 3 segments, each one being 1.6 m large (white rectangles on Figure 6). Each segment can be activated separately, allowing to modify the length of the gust. The experimentation were realized for a wind speed up to 2.5 m.s^{-1} for a maximum forward speed of the airship around 3.8 m.s^{-1}.

The data from the tracking system used in this experiment gives the speeds, position and angles at the reference setting point of the virtually reconstructed airship. In this experiment, this reference point is closed to the nose of the airship. Then, to compare the experimental results with the model the center of volume speeds and positions have to be computed from the original data.

To match the model with the experiment, the initial conditions used in the model were extracted from the experimental data. However, sometimes, the gust's entry not being clearly recorded, those initial conditions could not be exploited. Null initial conditions and control inputs ahead of the gust were then used to match the experiment.

The Figure 7 shows the comparison of the model with the experiment for a specific run. The displacements are given for the center of volume of the airship. The grey area corresponds to the time when the nose of the airship is in the gust. Here, the airship starts to enter the gust at the time $t = 0.4$ s but this run doesn't show the airship fully exiting the gust.

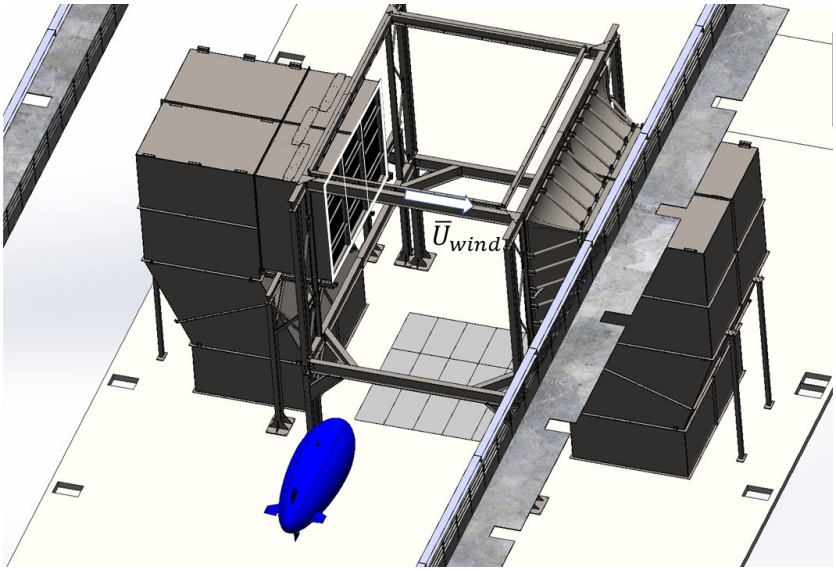

Fig. 6 ONERA's open windtunnel B20 used for the wind tests, Lille.

In this test, the initial conditions were extracted from the experiment. The main difference can be seen on the roll and pitch evolution. Indeed, it has already been explained that the roll and pitch oscillations were not perfectly described in the model.

Regarding the lateral displacement, it seems that the inertia of the airship in this direction is higher than it should be.

VII. Conclusion

This paper shows how a model was developed to describe the flight's dynamic of an airship, both in a calm atmosphere and through gust winds.

The model was confronted to several experiments through its development to test its different components. It shows the sensibility of airships to gust winds which can strongly interfere with the trajectory of an airship even with a rather low wind speed. This issue is mainly due to the complex balance of the mass for a buoyant object and the difficulty to fully control such an aircraft.

Further work could be done to test further the model thanks to experiments in order to make it reliable to predict trajectories in windy situations. Such development would be useful to allow the development of airships as replacement for helicopters or airplanes in specific contexts.

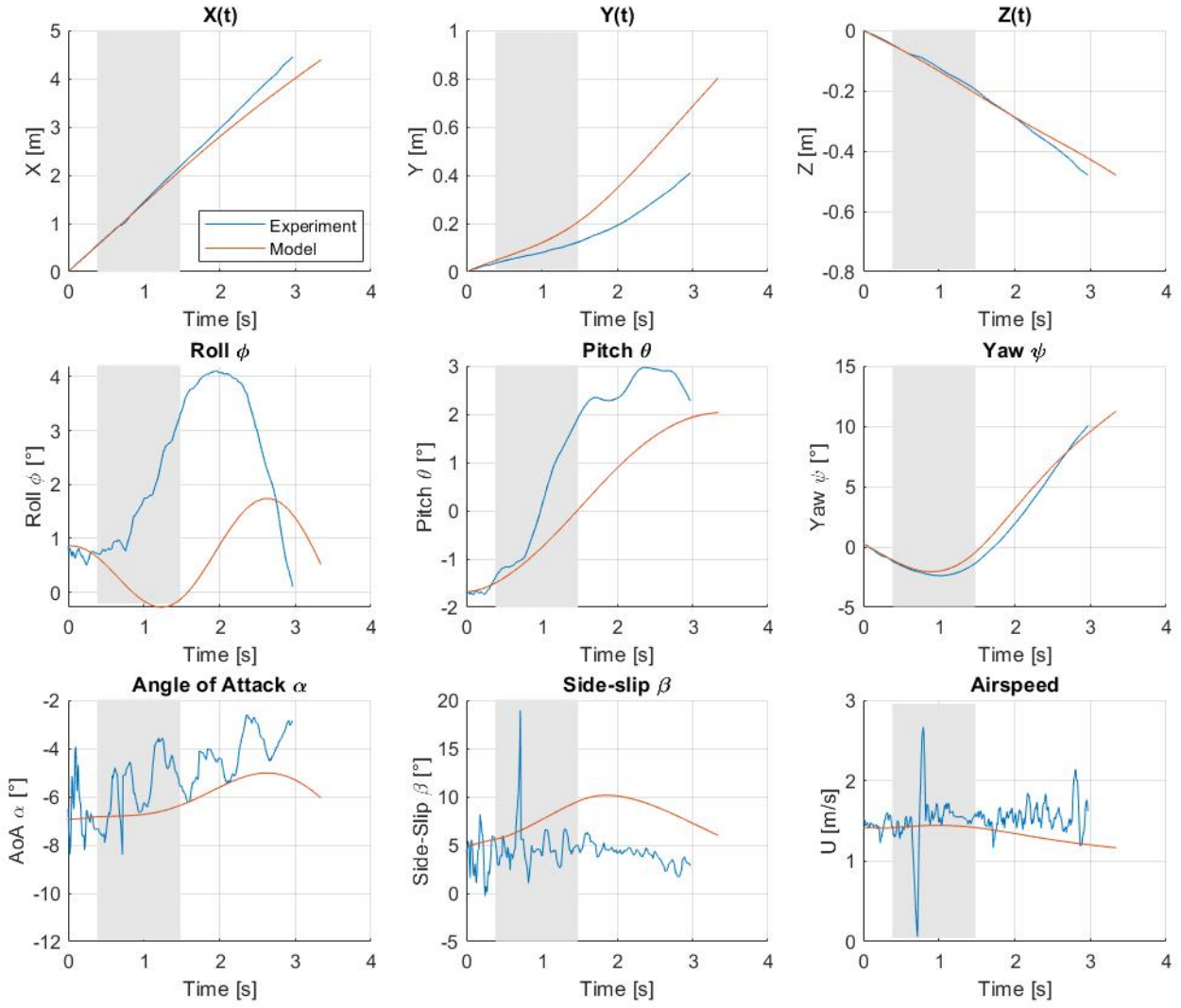

Fig. 7 Comparisons of the airship's trajectory through a 1 m.s^{-1} and 1.6 m long gust from the model and the experiment, positions expressed in the Earth's frame.

References

[1] Mueller, J.B., Paluszek, M.A., Zhao, Y. Development of an aerodynamic model and control law design for a high altitude airship, in: AIAA 3rd Unmanned Unlimited Technical Conference, Workshop and Exhibit, AIAA, Chicago, IL, 2004.

[2] Henderson, D. (1977). Shuttle Program. Euler angles, quaternions, and transformation matrices working relationships - NASA-TM-74839.

[3] Junkins, J., & Turner, J. (1986). *Optimal Spacecraft Rotational Maneuvers* (Vol. 3, Studies in Astronautics). Elsevier Science. pp. 31-34, table 2.2.

[4] Gomes, S.B.V. *An Investigation of the Flight Dynamics of Airships with application to the YEZ-2A*, PhD thesis, Cranfield Institute of Technology, Cranfield, 1990.

[5] Nakpiam, J. *Control of airship motion in the presence of wind*, Master Thesis, The University of Texas, Arlington, 2011.

[6] Bonnet, A. (1981). Introduction à un phénomène instationnaire: effets de masse et d'inertie ajoutée.

[7] Tuckerman, L.B. (1926). Inertia Factors of Ellipsoids for Use in Airship Design.

[8] Nielsen, J. (1988). *Missile aerodynamics.* Mountain View, Calif.: Nielsen Engineering & Research.

[9] Khoury, G.A. *Airship Technology - Second Edition*, Cambridge University Press, 2012.

[10] Li, Y., Nahon, M., & Sharf, I. (2011). Airship dynamics modeling: A literature review. *Progress in Aerospace Sciences*, 47(3), 217-239.

[11] Munson, B., Okiishi, T., & Young, D. (2006). *Fundamentals of fluid mechanics* (5.th ed.). Hoboken, N.J.: Wiley.

[12] Wardlaw, Andrew B. "High-Angle-of-Attack Missile Aerodynamics", *Missile Aerodynamics*, AGARD Lecture Series No. 98, Feb 1979, (pp 5-37, Fig 86).

[13] Ashraf, M., & Choudhry, M. (2013). Dynamic modeling of the airship with Matlab using geometrical aerodynamic parameters. *Aerospace Science and Technology, 25*(1), 56-64.

[14] Diederich, F. (1951). A plan-form parameter for correlating certain aerodynamic characteristics of swept wings.

[15] Li, Y. *Dynamics modeling and simulation of flexible airships*, PhD thesis, McGill University, Montreal, 2007.

[16] Ersdal, S., & Faltinsen, O. (2006). Normal forces on cylinders in near-axial flow. *Journal of Fluids and Structures*, 22(8), 1057-1077.

[17] Leishman, J. (2006). *Principles of helicopter aerodynamics - Second Edition* (Cambridge aerospace series). Cambridge: Cambridge University Press.

[18] Farcy, D. (2017). *Modélisation des effets de rafales: premiers developpements* (internal technical note), ONERA.

[19] Gong, A. & Verstraete, D., Development of a dynamic propulsion model for electric UAVs, *APISAT 2015 - 7th Asia-Pacific International Symposium on Aerospace Technology, 2015*, pp. 206-217.

[20] Wang, X., Fu, G., Duan, D., & Shan, X. (2010). Experimental Investigations on Aerodynamic Characteristics of the ZHIYUAN-1 Airship. *Journal of Aircraft, 47*(4), 1463-1468.